

The $^{14}\text{N} + ^{10}\text{B}$ system measured at $E(^{14}\text{N}) = 248$ MeV

M.E. ORTIZ, E.R. CHÁVEZ, A. DACAL

*Instituto de Física, Universidad Nacional Autónoma de México
Apartado postal 20-364, 01000 México D.F., México*

J. GÓMEZ DEL CAMPO
*Oak Ridge National Laboratory
Oak Ridge, TN 37831, USA*

Y.D. CHAN AND R.G. STOKSTAD
*Lawrence Berkeley Laboratory
Berkeley, CA 94720, USA*

Recibido el 14 de febrero de 1992; aceptado el 24 de marzo de 1992

ABSTRACT. Total and differential cross sections for reactions induced by ^{14}N on ^{10}B have been measured at a ^{14}N bombarding energy of 248 MeV (~ 18 MeV/A) for products from $Z = 3$ to 11. The study of saturation effects on the angular momentum and the identification of the non fusion cross sections constitute the aim of the present work. Energy, angular and Z distributions are presented and compared to Hauser-Feshbach calculations for the fusion components and a sum rule model for the non-fusion components. The extracted critical angular momentum is $21 \pm 2\hbar$ and is the same as at lower energies. The experimental total reaction cross section is in agreement with an optical model calculation.

RESUMEN. Se midieron secciones totales y diferenciales de reacciones inducidas por ^{14}N sobre ^{10}B a 248 MeV (~ 18 MeV/A), registrando productos desde $Z = 3$ hasta 11. El propósito de este trabajo es estudiar los efectos de saturación del momento angular así como identificar las secciones diferentes a la fusión. Se presentan distribuciones de energía, angulares y de carga (Z) y se comparan con cálculos Hauser-Feshbach para las componentes de fusión y con un modelo de regla de suma para las demás. El momento angular crítico extraído es de $21 \pm 2\hbar$, que es el mismo valor que a menores energías. La sección total de reacción concuerda con los cálculos de modelo óptico.

PACS: 25.70.-z; 25.70.Jj; 25.70.Gh

1. INTRODUCTION

It is well established that in heavy ion reactions of light systems ($A_T + A_P \leq 40$) at energies below 10 MeV/A fusion is the dominant mechanism. Complete fusion reactions consistent with an equilibrated compound nucleus have been measured for many systems in this energy region [1-8]. A review [9] has been published, based on the Glas-Mosel parameterization, indicating the importance of the behavior of σ_F at high energies in connection to the nucleus-nucleus potential. Nevertheless, at around or slightly above 10 MeV/A strong competition with incomplete fusion reactions appears [10], which could be responsible for the decreases in the fusion cross sections at high energies. In previous

publications [5,11,12] the proportionality of σ_F to $1/E_{cm}$ has been interpreted as a saturation of the maximum angular momentum (*e.g.*, the liquid drop limit) and with this idea in mind higher energy measurements for the $^{14}\text{N} + ^{10}\text{B}$ were made in order to understand the behavior of σ_F as well as the non fusion channels.

A pronounced difference in the behavior of the $^{14}\text{N} + ^{10}\text{B}$ and $^{12}\text{C} + ^{12}\text{C}$ systems for lower energies has been discussed in a previous work [12]. Compound nucleus limitations [13,14] on J_{cr} do not seem to be the limiting factor for $^{14}\text{N} + ^{10}\text{B}$ but could be for the $^{12}\text{C} + ^{12}\text{C}$ system, which apparently reaches the rotating liquid drop limit (RLD) [15].

In this work we have measured the evaporation-residue cross sections at a high energy to assure that we are in the region of saturation of J_{cr} . The expected fusion cross section for a J_{cr} value of $21 \hbar$, is ~ 500 mb but the increase of the total reaction cross section σ_R with bombarding energy makes the non-fusion component very important in this energy region (70% of σ_R). Due to the high excitation energy deposited in the compound nucleus (~ 132 MeV) the extraction of the fusion cross section by measuring the evaporation residues (*ER*) is difficult because they have nuclear charges (Z) lower than those of the target and/or projectile. However by a detailed study of the energy spectra it is possible to identify components other than complete fusion, which may be interpreted as contributions from incomplete fusion or direct reactions.

After describing the experiment in Sect. 2, we present the data in Sect. 3. Sect. 4 discusses experiment and calculations and Sect. 5 gives the conclusions.

2. EXPERIMENT

Measurements were performed at the Lawrence Berkeley Laboratory using a ^{14}N beam extracted from the 88-inch Cyclotron to bombard a self-supported enriched (99%) ^{10}B target of $128 \mu\text{g}/\text{cm}^2$ thickness.

Reaction products were detected with a solid state Si counter telescope consisting of two ΔE detectors with thicknesses of 10 and $75 \mu\text{m}$ and one E of $2000 \mu\text{m}$. The solid angle of the telescope was 2.4 msr. Angular distributions were measured from 4 to 38 degrees. Two solid state detectors were mounted symmetrically above and below the reaction plane to provide additional monitoring and relative normalization. For purposes of absolute normalization a second experiment was carried out using two position sensitive $\Delta E - E$ telescopes and a $175 \mu\text{g}/\text{cm}^2$ ^{10}B enriched target. The thickness of this target was determined by measuring the energy loss of α -particles from a ^{248}Cf source and by Rutherford scattering of protons at 700 keV. The total percentage of all contaminants did not exceed 6%. One of the telescopes was used as a monitor at 25 degrees and the other one ($\Omega = 0.3$ mrs) covered an angular range from 5 to 27 degrees. The estimated uncertainties of the cross sections were $\pm 10\%$.

3. EXPERIMENTAL RESULTS

Energy spectra ($d^2\sigma/d\Omega dE$) and energy-integrated angular distributions for the production of a fragment with a given nuclear charge Z , $(d\sigma/d\Omega)_Z$ were obtained. Experimental

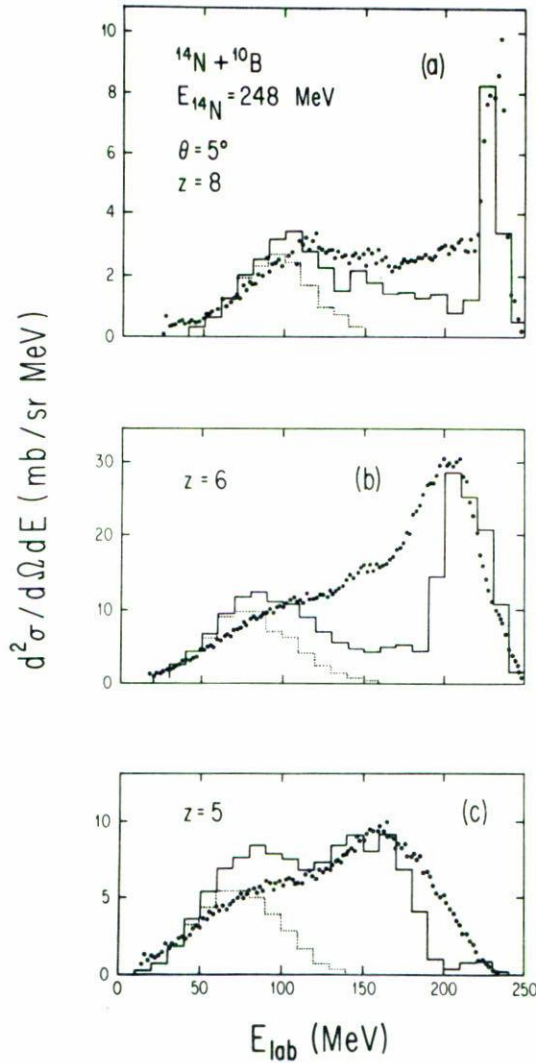


FIGURE 1. Energy spectra for $Z = 8$ (a), 6 (b) and 5 (c) at $E(^{14}\text{N}) = 248$ MeV at 5° . The solid line histograms are the sum of the Monte-Carlo calculations for fusion (dotted histograms) and non-fusion components discussed in the text.

results of the energy spectra, taken at 5° for fragments of $Z = 5, 6$ and 8 are shown in Fig. 1 by the dots. The solid histograms shown in this figure are the results of calculations of the total reaction cross sections and the dotted histograms correspond to the calculated evaporation residue spectra. Spectra for boron isotopes obtained for angles of 8 and 27 degrees are displayed in Fig. 2, where the histograms have the same meaning as in Fig. 1. The measured spectrum (dots) of carbon isotopes at 22 degrees is shown in Fig. 3 where also the calculations are given by the histograms. The main conclusion to be drawn from all these spectra is that the components higher in energy than the fusion one due to direct reaction and incomplete fusion, are very large and therefore a suitable deconvolution was carried out at every angle, thus permitting the separation of the fusion part.

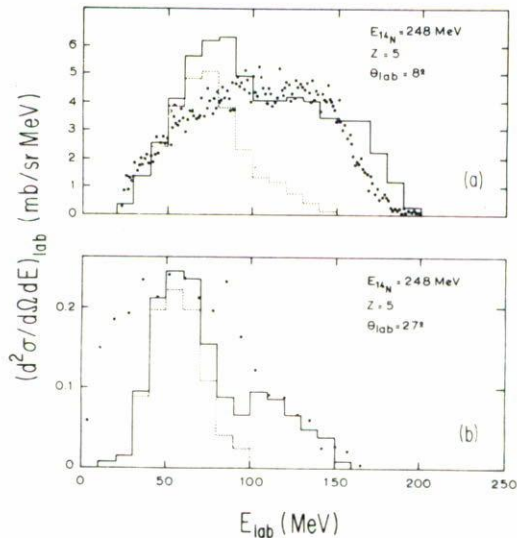


FIGURE 2. Energy spectra for boron ions at 8° (a) and 27° (b) taken at 248 MeV bombarding energy. These histograms have the same meaning as in Fig. 1.

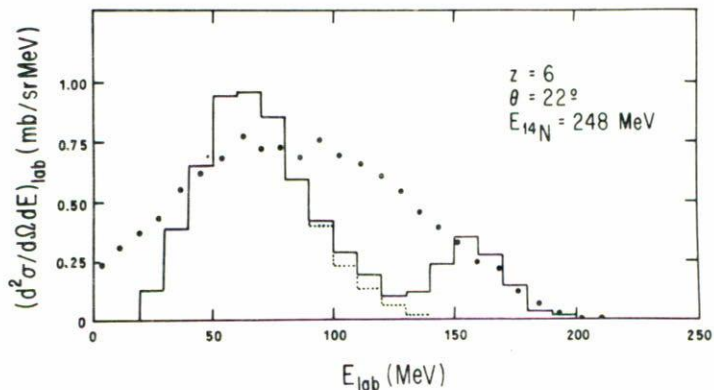


FIGURE 3. Energy spectrum of carbon at 22° and $E(^{14}\text{N}) = 248$ MeV. The histograms have the same meaning as in Fig. 1.

The deconvolution of the energy spectra into direct (high energies) and compound (lower energies) components was done simulating the shape of the ER spectra using the code LILITA [16] with a critical angular momentum of $21\hbar$ which is the value obtained at lower energies. The shape of the calculated ER spectra depends very little on the J_{cr} value.

Angular distributions of the total integrated spectra of O, C and B are plotted in Fig. 4. They are strongly forward peaked consistent with more direct reaction components. Contributions of the low energy recoiling partners are assumed to be negligible for angles smaller than 30°. The solid histograms are the sum of the LILITA calculations for the fusion cross sections plus the non-fusion cross sections calculated as described in Sect. 4. The total cross sections are obtained by integrating the angular distributions like those

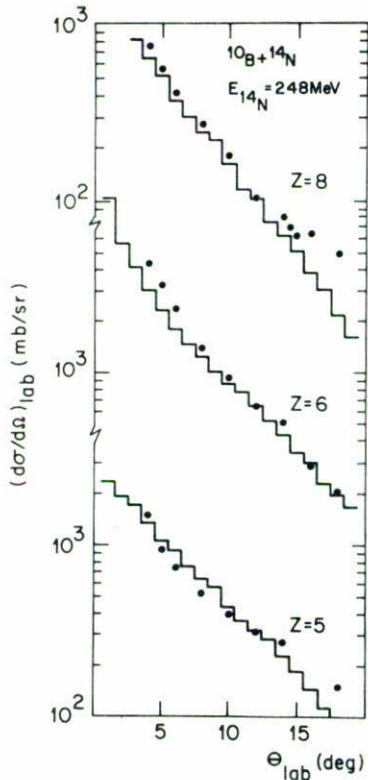


FIGURE 4. Angular distributions of the total cross section for oxygen, carbon and boron isotopes at 248 MeV. The solid histograms represent the Monte-Carlo calculations for the total reaction cross section as discussed in the text.

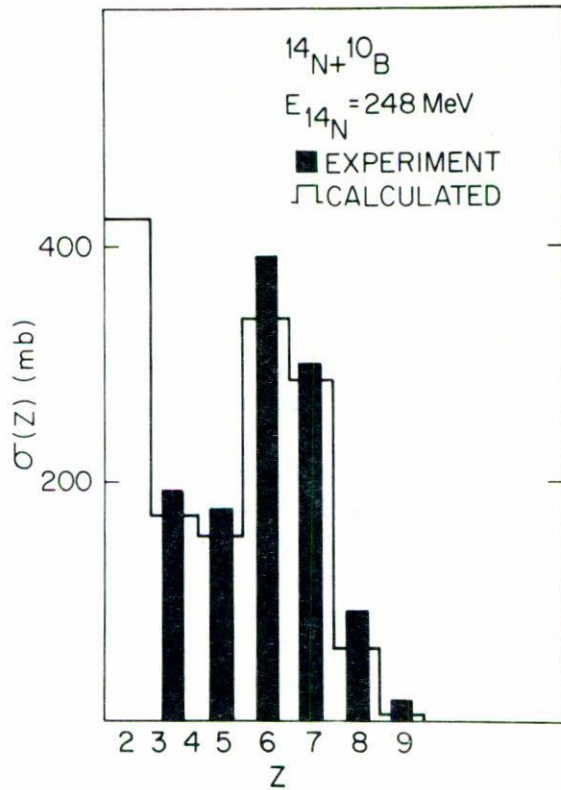


FIGURE 5. Total reaction cross sections in mb plotted against Z . The solid bars represent the experimental measurements and the histogram is the sum of the Monte-Carlo calculations of the fusion and non-fusion components.

TABLE I. Experimental total reaction cross sections (σ_R^{exp}), fusion (σ_F^{exp}). The theoretical non-fusion cross sections (σ_{NF}^{th}) was obtained by the Wilczynski sum-rule model plus the inelastic channel. The calculated total reaction cross section (σ_R^{th}) is the sum of σ_F^{exp} and σ_{NF}^{th} for each residue ($Z = 2-9$) in the $^{14}\text{N} + ^{10}\text{B}$ system. All cross sections are given in mb. The errors for the experimental quantities are $\pm 10\%$.

Z	2	3+4	5	6	7	8	9	σ_T
σ_R^{exp}	*	191	178	394	302	93	13	1171
σ_F^{exp}	*	66	72	145	119	24	1	427
σ_{NF}^{th}	328	106	83	196	166	35	2	920*
σ_R^{th}	424	172	155	341	285	59	3	1443*

*No measurements are available for $Z = 2$. See text for discussion of this yield.

shown in Fig. 4. Listed in the first row of Table I are the resulting experimental cross sections as a function of Z . The 2nd row of Table I contains the experimental fusion cross section determined by the deconvolution procedure previously described and the

third row shows the theoretical predictions of the total reaction cross sections for each Z . Fig. 5 shows the $\sigma_R(Z)$ distribution where the solid bars represent the experimental cross sections and the histogram the theoretical calculations for the sum of fusion and non-fusion components. To determine the total reaction cross section integrated over Z it is necessary to estimate the amount that produces residues down to $Z = 2$, since no experimental data is available for alpha particles in this experiment. The predicted alpha particle yield is 424 mb and is also plotted in Fig. 5, which added to the experimental values of σ_R given in the first row of Table I produces a total reaction cross section of 1595 mb. The calculation also predicts a 96 mb yield of residues of $Z = 2$, which added to the experimental σ_F values given in the second row of Table I produces a value of 523 mb. Using the sharp cut off approximation to σ_F , the extracted value of J_{cr} is $21\hbar$.

To determine the total reaction cross section, the elastic scattering of $^{14}\text{N} + ^{10}\text{B}$ was measured and the results plotted in Fig. 6 (dots). An optical model fit to these data was done and is shown by the solid line on the same figure. The parameters used in this fit are consistent with the behavior of the absorptive potential as a function of energy observed for this system at lower energies [12] with the same geometry and real potential. The resulting total reaction cross section is 1443 mb which compares favorably with the value of 1595 mb extracted experimentally.

4. CALCULATIONS AND DISCUSSION

In order to model the non-fusion cross section, which is almost 70% of the total reaction cross section, we start with a primary two-body collision followed by an in-flight evaporation of the excited fragments. We used the sum-rule model proposed by Wilczynski *et al.* [17] in an attempt to fix the characteristics of two-body stage, and then, to simulate the decay of the excited primary fragments, the two-body version of code LILITA [16,18] was used. Also an inelastic scattering channel that is not included in the Wilczynski's model was incorporated empirically. In addition the evaporation residues were simulated using a J_{cr} of $21\hbar$ as mentioned previously.

Wilczynski's sum-rule model accounts for all possible transfers going from projectile to target and vice versa. Thus it encompasses deep inelastic collisions (few nucleon transfer) and incomplete fusion (massive transfer); these processes have been invoked before to analyze similar systems in this energy region [19–21].

In the case of nearly symmetric systems the transfer of nucleons in both directions is comparable, and the excitation energies associated with each partition should be shared somehow between the target and the projectile-like fragments. The way this sharing should be done is not clear up to now [17,22,23,24]. For this light system we feel that the most reasonable assumption is that the excited fragment is the one that receives the transferred nucleons, no matter which partner it is, this may introduce some difficulties for symmetric channels but is obviously correct for massive transfers.

The sum-rule model contains three free parameters, the effective Coulomb interaction radius R , the effective temperature T and the diffuseness of the transmission coefficient distribution Δ . They were fixed by fitting the measured fusion cross sections at six different

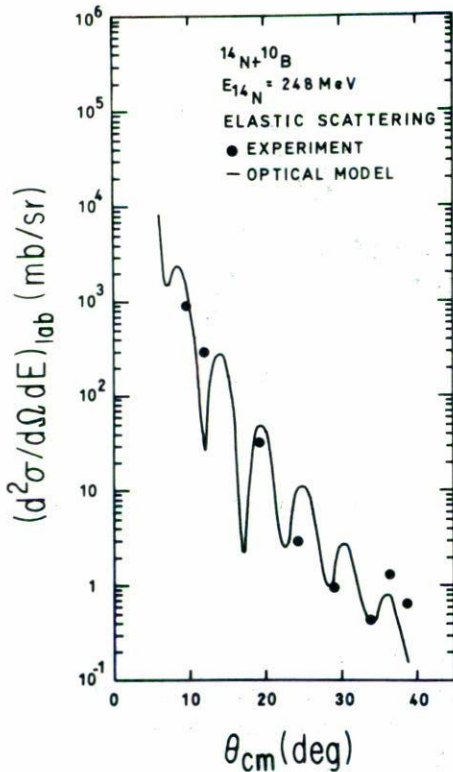


FIGURE 6. Elastic scattering angular distribution for $^{14}\text{N} + ^{10}\text{B}$ system at $E(^{14}\text{N}) = 248$ MeV. The solid curve represents the optical model fit calculated with the following parameters for the real potential: $V = 23.614$ MeV, $r_0 = 1.25$ fm, and $a_0 = 0.52$ fm; and for the imaginary part $W = 24.23$ MeV, $r_0 = 1.22$ fm, and $a_0 = 0.54$ fm. The Coulomb radius $r_0 = 1.3$ fm.

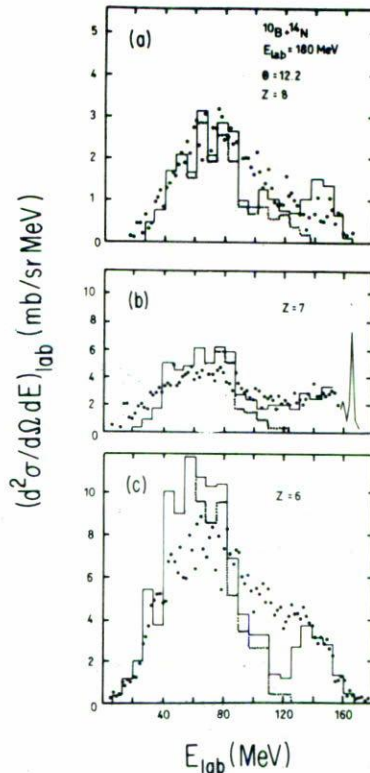


FIGURE 7. Energy spectra for oxygen (a), nitrogen (b) and carbon (c) isotopes at 180 MeV and 12.2° . The meaning for the histograms are the same as in Fig. 1.

energies from $E = 86$ up to 248 MeV with a fixed set of values ($r = 1.5$ fm, $T = 4.8$ MeV and $\Delta = 1.5$). To set this fit, it was necessary to use a different expression for the half density radii C than that given by Wilczynski [25]. The expression that we used was $C = 1.18 A^{1/3}$.

The Q -value distribution for each channel is introduced in the evaporation code as a gaussian distribution centered at an excitation energy (E_x) estimated as the difference between Q_{opt} [17] and Q_{gg} with the cross section and optimum J predicted by Wilczynski's model and the J distribution function given in Ref. [16]. This model does not account for the inelastic channel (no particle transfer). Therefore we simulate this channel using a Q -value exponential distribution and estimating its cross section by the integration of the angular distribution obtained for nitrogen ($E_x = 18$ –70 MeV). A listing of all contributing channels is shown in Table I.

The original Wilczynski model is not adequate for the description of nearly symmetric systems [17,22], however in the present work we have used the model with significant

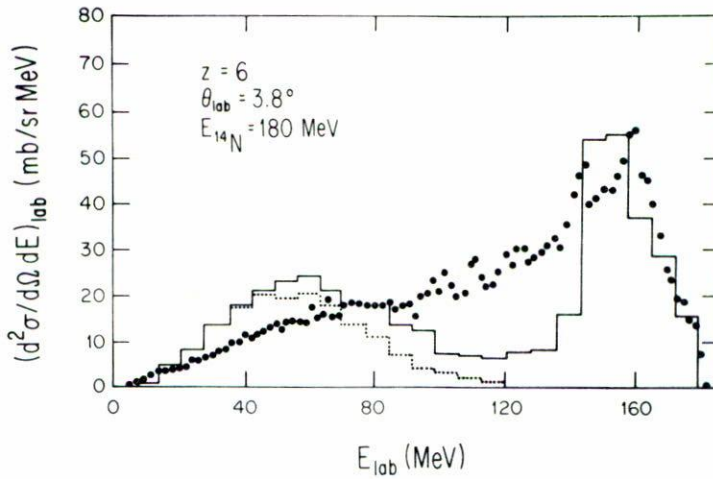


FIGURE 8. Energy spectrum for $Z = 6$ at 3.8° and $E(^{14}\text{N}) = 180$ MeV. The histograms have the same meaning as in Fig. 1.

modifications needed to describe our fusion and inelastic scattering data. The main features of the calculations can be appreciated in Figs. 1 to 3 by the solid histograms; in all of them the lower energy group corresponds to the fusion evaporation residues and the higher energy group results from the modified Wilczynski model just described. It is important to notice that the cross sections are absolute with no arbitrary normalization factor. It can be seen from all these figures that the relative contributions from direct and compound components are rather well reproduced, although notable discrepancies can be seen in the shape of the spectra like for $Z = 6$ in Figs. 6 and 7.

Since data for the $^{14}\text{N} + ^{10}\text{B}$ system are available at lower energies [12], the calculations were repeated at 86 and 180 MeV. As expected, the binary-reaction cross sections are almost negligible at 86 MeV. The results at 180 MeV where the two-body reaction cross sections start to be important are plotted for $Z = 6, 7$ and 8 at 12° in Fig. 7. Fig. 8 shows the carbon spectrum at 3.8° with the same convention for the histograms as before. As can be seen it is encouraging that the description is better than at 248 MeV.

Although measurements of fusion-like cross sections at high energy above 10 MeV/A are difficult, they are of fundamental importance in establishing basic properties of nuclear collisions like critical angular momentum, nuclear disassembly and nuclear matter equation of state [26]. In particular the disappearance of the fusion-like residues [26] are important measurements in the determination of the equation of state. The compilation of all the $^{14}\text{N} + ^{10}\text{B}$ measurements is given in Fig. 9. The open circles correspond to the measurements discussed in Ref. [12], except for the point at 18 MeV/nucleon which corresponds to the present work. The solid line is the result of a theoretical calculation using the reaction parameters given by Wilcke *et al.* [27], but with a J_{cr} value of $21\hbar$ consistent with the experiment. The J_{cr} value given in Ref. [27] for this system is $19\hbar$. As can be seen from Fig. 9 the calculation reproduces the data at high energies, thus indicating that up to 18 MeV/nucleon the limitation on the fusion cross section for $^{14}\text{N} + ^{10}\text{B}$ is consistent with critical angular momentum effects.

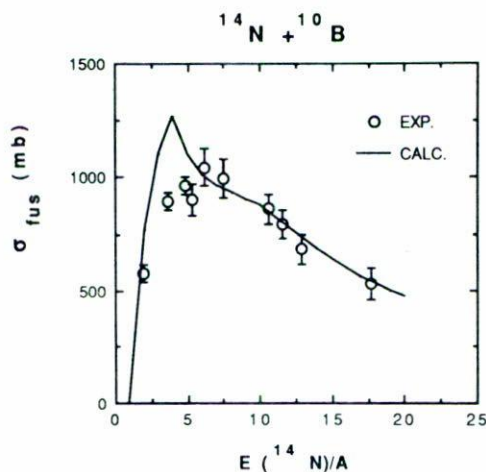


FIGURE 9. Experimental fusion cross section (points) compared to a calculation (line) with J_{cr} value of $21\hbar$.

5. CONCLUSIONS

We have measured complete energy spectra for all reaction products from $Z = 3$ to 11 at several angles between 4 and 38 degrees. At this high bombarding energy (~ 18 MeV/A), the separation between direct and compound components is not as evident as at lower energies; however with the procedure used to describe the total reaction cross section, this separation is still possible.

The application of the sum-rule model to the non-fusion component has to be considered as a first approximation and the problem of taking into account mutual excitations of both fragments must be solved for this kind of system. Nevertheless the model exhibits encouraging features up to 18 MeV/A.

The set of data for this system at 103 MeV center-of-mass energy presented here provides a new indication of the saturation of $J_{cr} \sim 21\hbar$. This supports the conclusions of previous work [12]. The estimate of the non fusion cross section is based on our confidence in the Monte-Carlo Hauser Feshbach calculations coupled to the modified Wilczynski model.

ACKNOWLEDGEMENTS

We are very grateful to the staff members of the LBL 88-inch Cyclotron for their hospitality and help during the experiments. Valuable discussions with R. Dayras are also acknowledged. We also thank K. Lopez for the operation of the 700 keV accelerator. This work was partially supported by CONACYT (Mexico) under contracts PCCBBNA-022683 and PC228CC0X-880237. Oak Ridge National Laboratory is managed by Martin Marietta Energy Systems Inc. under contract No. DE-AC05-84OR21400 with the U.S. Department of Energy. The work of Y. Chan and R. Stokstad was supported by the office of High Energy and Nuclear Physics and by the Nuclear Sciences of Basic Energy Sciences program of the U.S. Department of Energy under contract No. DE-AC03-765F00098.

REFERENCES

1. M.N. Namboodiri, E.T. Chulick and J.B. Natowitz, *Nucl. Phys.* **A263** (1976) 491.
2. D. Horn, A.J. Ferguson and O. Hauser, *Nucl. Phys.* **A311** (1978) 328.
3. J. Gómez del Campo, D.E. DiGregorio, J.A. Biggerstaff, Y.D. Chan, D.C. Hensley, P.H. Stelson, D. Shapira and M.E. Ortiz, *Phys. Rev.* **C35** (1987) 137.
4. J. Gómez del Campo, R.A. Dayras, J.A. Biggerstaff, D. Shapira, A.H. Snell, P.H. Stelson and R.G. Stokstad, *Phys. Rev. Lett.* **43** (1979) 26.
5. J. Gómez del Campo, R.G. Stokstad, J.A. Biggerstaff, R.A. Dayras, A.H. Snell and P.H. Stelson, *Phys. Rev.* **C19** (1979) 2170.
6. R.L. Parks, S.T. Thornton, L.C. Dennis and K.R. Cordell, *Phys. Rev.* **A348** (1980) 350.
7. C. Beck, F. Hass, R.M. Freeman, B. Heusch, J.P. Coffin, G. Guillaume, F. Rami and P. Wagner, *Phys. Rev.* **C29** (1984) 1942.
8. J.F. Mateja, A.D. Frawley, D.G. Kovar, D. Henderson, H. Ikezoe, R.V.F. Janssens, G. Rosner, G.S.F. Stephans, B. Wilding, K.T. Lesko and M.F. Vineyard, *Phys. Rev.* **C31** (1985) 867.
9. J. Gómez del Campo and G.R. Satchler, *Phys. Rev.* **C28** (1983) 952.
10. H. Morgenstern, W. Bohne, W. Galster, K. Grabish and A. Kyanowski, *Phys. Rev. Lett.* **52** (1984) 1104.
11. J. Gómez del Campo, J.A. Biggerstaff, R.A. Dayras, D. Shapira, A.H. Snell, P.H. Stelson and R.G. Stokstad, *Phys. Rev.* **C29** (1984) 1722.
12. M.E. Ortiz, J. Gómez del Campo, Y.D. Chan, D.E. DiGregorio, J.L.C. Ford, D. Shapira, R.G. Stokstad, J.P.F. Sellschop, R.L. Parks and D. Wisner, *Phys. Rev.* **C25** (1982) 1436.
13. R. Vandenbosch and J. Lazzarini *Phys. Rev.* **C23** (1981) 1074.
14. S.M. Lee, T. Matsuse and A. Arima, *Phys. Rev. Lett.* **45** (1980) 165.
15. S. Cohen, *Ann. Phys. (NY)* **82** (1974) 557.
16. J. Gómez del Campo and R.G. Stokstad, Oak Ridge National Laboratory Technical Memo. No. ORNL-TM-7295 (1974).
17. J. Wilczynski, S. Siwek-Wilczynska, J. Van Driel, S. Gongrijp, D.C.J.M. Hageman, R.V.F. Janssens, J. Lukasiak, R.H. Siemssen and S.Y. Van Der Werf, *Phys. Rev.* **A373** (1982) 109.
18. J. Gómez del Campo, *Proceedings of the Symposium on Heavy Ion Physics from 10 to 200 MeV/amu held at Brookhaven National Laboratory*. July 16-20 (1979).
19. R.Y. Cusson, J. Gómez del Campo, J.A. Maruhn and V. Maruhn-Rezwany, *Phys. Rev.* **C23** (1981) 2524.
20. A. Menchaca-Rocha, M.E. Brandan, A. Dacal, A. Galindo, J. Mahoney, M. Murphy and W.D.M. Rae, *Phys. Letters* **121B** (1983) 111.
21. Y.D. Chan, M. Murphy, R.G. Stokstad, I. Tserruya, S. Wald and A. Budzariowski *Phys. Rev.* **C27** (1983) 447.
22. J.P. Bondorf, F. Dickman, D.H.E. Gross and P.J. Siemens, *J. de Phys. Coll.* **32, C6** (1971) 145.
23. J. Wilczynski and K. Siwek-Wilczynska, *Phys. Rev.* **C41** (1990) 1917.
24. S. B. Gazes, H. R. Schmidt, Y. Chan, E. Chavez, R. Kamerans and R.G. Stokstad, *Phys. Rev.* **C38** (1988) 712.
25. J. Wilczynski, *Nucl. Phys.* **A216** (1973) 386.
26. H.M. Xu, W.G. Lynch, P. Danielewicz and G.F. Bertch, *Phys. Rev. Lett.* **65** (1990) 843.
27. W.W. Wilke, J.R. Birkelund, H.J. Wollershein, A.D. Noover, J.R. Huizenga, W.V. Shroeder and L.E. Tubbs, *Atomic and Nuclear Data Tables* **25** (1980) 391.